Biaxiality of chiral liquid crystals

Lech Longa*
International Centre for Theoretical Physics, P.O. Box 586, 34100 Trieste, Italy
and Department of Statistical Physics, Jagellonian University, Reymonta 4, Kraków, Poland

Werner Fink and Hans-Rainer Trebin
Institut für Theoretische und Angewandte Physik, Universität Stuttgart, Pfaffenwaldring 57, Germany
(Received 10 January 1994)

Using the extended de Gennes–Ginzburg–Landau free energy expansion in terms of the anisotropic part $Q_{\alpha\beta}(\boldsymbol{x})$ of the dielectric tensor field, a connection between the phase biaxiality and the stability of various chiral liquid crystalline phases is studied. In particular, the cholesteric phase, the cubic blue phases, and the phases characterized by an icosahedral space group symmetry are analyzed in detail. Also, a general question concerning the applicability of the mean-field approximation in describing the chiral phases is addressed. By an extensive study of the model over a wide range of the parameters, a class of phenomena, not present in the original de Gennes–Ginzburg–Landau model, has been found. These include (a) reentrant phase transitions between the cholesteric and the cubic blue phases and (b) the existence of distinct phases of the same symmetry but of different biaxialities. The phase biaxiality serves here as an extra scalar order parameter. Furthermore, it has been shown that, due to the presence of competing bulk terms in the free energy, the stable phases may acquire a large degree of biaxiality, also in liquid crystalline materials composed of effectively uniaxial molecules. A study of icosahedral space group symmetries provides a partial answer to the question of whether or not an icosahedral quasicrystalline state can be stabilized in liquid crystals. Although, in general, the stability of icosahedral structures could be enhanced by the extra terms in the free energy, no absolutely stable icosahedral phase has been found.

PACS number(s): 64.70.Md, 05.70.Ce, 61.30.−v, 61.50.Em

I. INTRODUCTION

Chirality is today considered as one of the most important and complex research topics in liquid crystal physics. It not only leads to phases of a great technological interest, such as polar smectic-C^*, but also gives rise to unusual structures known as blue phases [1,2]. These, which will be of our concern, are thermodynamically stable in a narrow temperature range ($\sim 0.1-5$ K) between the isotropic liquid phase (ISO) and the cholesteric phase (Ch). At present there are seven blue phases known of which three appear under condition of zero electric field, being labeled, in order of increasing temperature, BPI, BPII, and BPIII.

The crucial parameter governing the stability of chiral phases is the pitch (or its inverse, the chirality). In systems of large pitch (small chirality), typically greater than 5000 Å, only a direct ISO-Ch phase transition is detected. As pitch is decreased, an ISO-BPI-Ch sequence of phases is first observed, which next is replaced by an ISO-BPII-BPI-Ch sequence. As still higher chirality, the BPIII phase appears on the phase diagram between ISO and BPII phases. For sufficiently small pitch ($\sim$ 1500 Å), the BPII phase disappears completely. The transformations between the phases are of first order.

Experiments conducted to date show that BPI and BPII may be described as a body-centered-cubic structure with space group symmetry of $O^8(I4_132)$ and a simple cubic structure with space group symmetry $O^2(P4_232)$, respectively. The three-dimensional cubic order is acquired by the mean molecular orientations yielding circularly polarized Bragg reflections of visible and uv light. Contrary to ordinary crystals the centers of mass of the molecules are assumed to be positionally disordered, like in an isotropic liquid. But so far this hypothesis has not been proven experimentally.

The present theoretical models correctly describe the order of the phase transitions between ISO, Ch, BPI, and BPII. Also the cubic structures emerge from the calculations with lowest free energies. But other features of the phase diagrams, such as, for example, a restricted stability domain of BPII, remain unexplained.

The structure of BPIII, which is formed directly on cooling the isotropic liquid, is still a matter of intensive studies. It has many features common with the cubic BP (thermodynamic stability, lack of birefringence, and strong optical activity), but does not exhibit Bragg scattering. Instead, a broad selective reflection band, typical of an amorphous system [1,3,4], is observed. These experimental observations have recently been proposed to result from a cubic bond orientational order — the only long-range order expected in BPIII [5].

But there are two concurrent models for the structure of BPIII [1,5–7], the most intriguing among them being

*Electronic address: lechifuj@jetta.if.uj.edu.pl

the *icosahedral model.* It assumes that BPIII possesses the quasiperiodic symmetry of an icosahedral quasicrystal. The absence of a quasicrystalline pattern in light diffraction is attributed to a destructive character of phason degrees of freedom [6]. In the liquid state they may prevent the growth of single quasicrystallites, several micrometers in size, necessary to resolve closely positioned icosahedral peaks.

While experiments still are not fully conclusive, there is a serious theoretical difficulty with the icosahedral model: The de Gennes–Ginzburg–Landau (deGL) theory of liquid crystals [8], which has proven successful in describing structural properties of BPI and BPII [1], shows that in the physically relevant chirality range the quasicrystalline order is always less stable than the cholesteric and the cubic structures involved. A detailed stability analysis of the quasicrystalline order within the frame of an extended model [7] yields similar predictions, at least in the vicinity of the isotropic liquid.

Despite these negative results for the structure of BPIII a general idea concerning stabilization of an icosahedral chiral liquid crystal seems very intriguing and certainly deserves further considerations. If an icosahedral structure would appear as a stable liquid state (not necessarily BPIII), its physical properties are expected to be quite different from those of metallic quasicrystals [9]. For example, it seems that such a liquid crystal is a perfect system for studying the physics of phasons. Unlike in metallic quasicrystals [9], where phasons form a quenched positional disorder, in liquid crystals they would form an annealed orientational disorder. This in turn may strongly inhibit growth of single quasicrystallites and influence relaxation and surface phenomena.

As a number of important problems are still left unsolved in the frame of the de Gennes–Ginzburg–Landau theory [1,5–7], it is our objective here to analyze some within the frame of the more general extended de Gennes–Ginzburg–Landau (EdeGL) theory, which applies to a wider class of liquid crystalline materials. Results will be discussed in terms of a new scalar order parameter, the phase biaxiality, which characterizes "the degree of twisting" of a chiral structure. With the help of this parameter the roles played by various terms in the EdeGL theory will be clarified. Next, classes of phase diagrams are established that could be relevant to the presently existing experimental data. Finally, a detailed analysis of the stability of icosahedral structures will be carried out by comparing their free energies with those of Ch, BPI, BPII, and the O^5(I432) structures. While our previous studies [7] were basically restricted to a neighborhood of the isotropic phase, the calculations presented here cover all relevant ranges of chirality and temperature.

The organization of the paper is as follows. In Sec. II the extended de Gennes–Ginzburg–Landau theory is introduced in a more general thermodynamic context. Section III is concerned with details of the free energy calculations for periodic and quasiperiodic structures. In Sec. IV results of the numerical analysis are discussed and possible classes of phase diagrams are identified. Section V contains a short summary.

II. EXTENDED de GENNES–GINZBURG–LANDAU THEORY

The transition between liquid crystalline phases can be described in different length scales. For the cholesteric phase and for the blue phases of chiral liquid crystals the characteristic dimension associated with the structure is of the order of 4000 Å. Consequently, the relevant length scale is the mesoscopic one, where the difference in the order of the molecules is best quantified in terms an order parameter. It represents the extent to which the average configuration of the molecules in the less symmetrical phase differs from that in the more symmetrical one.

In general, many order parameters are needed to characterize translational and orientational properties of a liquid crystal. However, a unique order parameter set may always be divided into primary order parameters and secondary ones. In equilibrium the secondary order parameters are functionals of the primary ones. A standard way of detecting the primary order parameters is by referring to the one-particle distribution function or to the macroscopic response functions of the bulk material [8].

In the absence of long-range correlations between the centers of mass of the molecules the primary order parameter describing liquid crystals is a symmetric and traceless tensor field $\boldsymbol{Q}(\boldsymbol{r})$ of Cartesian components $Q_{\alpha\beta}$ $(\alpha,\beta = x,y,z)$. The SO(3)-symmetric isotropic phase corresponds to the case when three eigenvalues of $\boldsymbol{Q}(\boldsymbol{r})$ are equal. Due to the vanishing trace condition this yields $\boldsymbol{Q}(\boldsymbol{r}) \equiv \boldsymbol{0}$. For the D_∞-symmetric uniaxial phases two out of the three eigenvalues of $\boldsymbol{Q}(\boldsymbol{r})$ are equal. In the case of the general, D_2-symmetric biaxial phase $\boldsymbol{Q}(\boldsymbol{r})$ has three different eigenvalues. The spatial dependence of $\boldsymbol{Q}$ takes into account a possibility of nonuniform configurations of the orientational degrees of freedom.

In statistical field theory $\boldsymbol{Q}(\boldsymbol{r})$ has the status of a random field and a general free energy F is defined as a Feynman integral of a functional $\mathcal{F}[\boldsymbol{Q}(\boldsymbol{r}),\partial\boldsymbol{Q}(\boldsymbol{r})]$ over all fields $\boldsymbol{Q}(\boldsymbol{r})$

$$F[\boldsymbol{Q}(\boldsymbol{r})] = -k_B\mathcal{T}\ln\int\mathcal{D}\,\boldsymbol{Q}(\boldsymbol{r})\exp\left\{\frac{-\mathcal{F}\,[\boldsymbol{Q}(\boldsymbol{r}),\partial\boldsymbol{Q}(\boldsymbol{r})]}{k_B\mathcal{T}}\right\}, \tag{2.1}$$

where $\mathcal{T}$ is the absolute temperature. The only restriction on $\mathcal{F}$ is that it must be (a) SO(3) symmetric and (b) stable against an unlimited growth of both $\boldsymbol{Q}(\boldsymbol{r})$ and $\partial\boldsymbol{Q}(\boldsymbol{r})$.

Two theorems [8], related to the intrinsic symmetry of $\boldsymbol{Q}(\boldsymbol{r})$, are important when an analytical expression for $\mathcal{F}$ is constructed. The first one states that any analytical SO(3)-symmetric function of $\boldsymbol{Q}(\boldsymbol{r})$ depends on two invariants only: $\mathrm{tr}(\boldsymbol{Q}^2)$ and $\mathrm{tr}(\boldsymbol{Q}^3)$. The second theorem is the inequality

$$\{\mathrm{tr}[\boldsymbol{Q}(\boldsymbol{r})^2]\}^3 - 6\{\mathrm{tr}[\boldsymbol{Q}(\boldsymbol{r})^3]\}^2 \geq 0, \tag{2.2}$$

where the equality holds for locally isotropic or uniaxial fields $\boldsymbol{Q}(\boldsymbol{r})$ [8]. The condition (2.2) becomes a strong inequality for locally biaxial (oblate or prolate) configurations. For fixed $\mathrm{tr}[\boldsymbol{Q}(\boldsymbol{r})^2]$ the biaxiality of a configura-

tion increases with decreasing value of $\{\mathrm{tr}[\boldsymbol{Q}(\boldsymbol{r}]^3]\}^2$ and approaches its maximal value for $\mathrm{tr}[\boldsymbol{Q}(\boldsymbol{r})^3] = 0$. The last observation suggests that any equilibrium structure, described in terms of $\boldsymbol{Q}(\boldsymbol{r})$, could be characterized *globally* by an SO(3)-invariant parameter

$$B = \overline{\left[\frac{\int d^3\boldsymbol{x}\,\{[\mathrm{tr}(\boldsymbol{Q}^2)]^3 - 6\,[\mathrm{tr}(\boldsymbol{Q}^3)]^2\}}{\int d^3\boldsymbol{x}\,[\mathrm{tr}(\boldsymbol{Q}^2)]^3}\right]}, \qquad (2.3)$$

where the $\overline{[]}$ denotes the thermodynamic average over the fields $\boldsymbol{Q}(\boldsymbol{r})$ with the exponential weight as introduced in Eq. (2.1). Configurations of $\int d^3\boldsymbol{x}\ \mathrm{tr}\,[\boldsymbol{Q}(\boldsymbol{r})^2]^3 = 0$ are excluded from (2.3). Note that for purely uniaxial phases B is minimal and equals zero while for phases of maximal biaxiality B approaches its maximal value 1. In this sense B is a scalar, normalized, and positive definite measure of biaxiality for an arbitrary equilibrium liquid crystalline phase or the *phase biaxiality* for short.

Though the definition (2.3) follows in a natural way from the symmetry of $\boldsymbol{Q}$, and as such is independent of $\mathcal{F}$, the calculations (2.1) require a specific form of $\mathcal{F}$. de Gennes [10] was the first to formulate a Landau-Ginzburg free-energy functional as expansion in terms of $\boldsymbol{Q}(\boldsymbol{r})$ and its derivatives $Q_{\alpha\beta,\gamma}$. The original expansion, also known as de Gennes–Ginzburg–Landau theory, was taken to the second order in the gradient $\partial_\mu \boldsymbol{Q}$ of the order parameter and to the fourth order in $\boldsymbol{Q}$. By introducing suitable units of energy, length, and $\boldsymbol{Q}$ [11] and in the absence of external fields it reads [8]

$$\begin{aligned}\mathcal{F} &\equiv \mathcal{F}_{\mathrm{deGL}}[\boldsymbol{Q}(\boldsymbol{r})] \\ &= v^{-1}\int d^3\boldsymbol{x}\left\{\frac{1}{4}\,[T\,\mathrm{tr}(\boldsymbol{Q}^2) - 2\,\kappa\,\varepsilon_{ijk}\,Q_{in}\,Q_{jn,k} \right. \\ &\quad + (Q_{ij,l})^2 + \rho\,Q_{ij,j}^2] \\ &\quad \left. -\sqrt{6}\,\beta\,\mathrm{tr}(\boldsymbol{Q}^3) + \gamma[\mathrm{tr}(\boldsymbol{Q}^2)]^2\right\}. \qquad (2.4)\end{aligned}$$

Here v is the volume of the system and ε_{ijk} is the Levi-Civita tensor. Also the Einstein summation convention over repeated indices is to be applied if not stated otherwise. The κ term in Eq. (2.4) is denoted chiral. It is crucial for the existence of stable chiral liquid crystals. Since it violates parity its presence in the expansion is responsible for the formation of phases of broken chiral symmetry, e.g., cholesteric or the blue phases.

The functional (2.4) depends only on three parameters: the reduced temperature T, the reduced chirality κ, which is proportional to the wave vector of the cholesteric phase, and the relative elastic constant ρ. The remaining two parameters β and γ are redundant. The parameter β is a dimensionless measure of the molecular flatness giving $\beta > 0$ for rodlike molecules and $\beta < 0$ for the disklike ones [8]. For $\mathcal{F}_{\mathrm{deGL}}$ to be positive definite requires that $\rho > -3/2$ and $\gamma > 0$. Due to the choice of units and due to the prolate-oblate symmetry of $\mathcal{F}_{\mathrm{deGL}}$ one may take $\beta = \gamma = 1$ [13].

A qualitative description of uniaxial nematics and cholesterics in the vicinity of the isotropic phase is accounted for by the expansion (2.4). But, as summarized below, a more complicated functional with higher-order terms in $\boldsymbol{Q}$ is actually needed to describe equilibrium properties of real systems.

First we note that the phase transitions involving chiral states are first order. Thus the higher-order terms may play an important role. Second, as shown in [8], the experimental data for nematics fit very well to a model with a sixth-order term in $\boldsymbol{Q}$ being dominant. As the presence of chirality is not expected to change the phenomenological parameters significantly this suggests that a physically relevant sector exists in the extended parameter space, which is not accessible within the original de Gennes model (2.4). Following this idea we consider a more general functional up to sixth order in $Q_{\alpha\beta}$ [8]. Again in the units of Grebel *et al.* [11] it reads [7,8]

$$\begin{aligned}\mathcal{F} &\equiv \mathcal{F}_{\mathrm{EdeGL}} \\ &= \mathcal{F}_{\mathrm{deGL}} + \frac{1}{v}\int \mathrm{d}^3\mathbf{x}\left\{-\frac{1}{\sqrt{6}}\phi[\mathrm{tr}(\boldsymbol{Q}^2)][\mathrm{tr}(\boldsymbol{Q}^3)]\right. \\ &\quad \left. + \frac{1}{6}\varepsilon[\mathrm{tr}(\boldsymbol{Q}^2)^3] + \frac{1}{6}\varepsilon'\{[\mathrm{tr}(\boldsymbol{Q}^2)^3] - 6[\mathrm{tr}(\boldsymbol{Q}^3)^2]\}\right\}, \qquad (2.5)\end{aligned}$$

where for $\gamma \le 0$, the inequality $\varepsilon' > -\varepsilon$ must be fulfilled for stability. For $\gamma > 0$ the expansion (2.5) is stable provided that $\varepsilon' \ge -\varepsilon$. Two out of five material parameters $(\beta, \gamma, \phi, \varepsilon, \varepsilon')$ are redundant [11] and can be set equal to 0 or ± 1.

Note that the higher-order bulk terms (2.5) have been written in such a way that for locally uniaxial structures the sixth order term, weighted by ε', vanishes [see Eq. (2.2)]. It becomes greater than zero in the presence of locally biaxial configurations. Thus for $\varepsilon' > 0$ the model characterizes liquid crystalline materials composed of (effectively) uniaxial molecules, while for $-\varepsilon < \varepsilon' < 0$ it describes liquid crystals of biaxial molecules [8].

A full thermodynamic description of chiral biaxial liquid crystals as represented by Eqs. (2.1) and (2.4) or by Eqs. (2.1) and (2.5) proves rather difficult. The major complication is due to the presence of the chiral term in $\mathcal{F}$. To date only partial mean-field results are known for the simpler case as represented by Eqs. (2.1) and (2.4). A purpose of this paper is to go one step further and carry out the mean-field analysis for the second, more complicated, theory.

We start by introducing the mean-field approximation. It is strictly related to the way the Feynman integral (2.1) and (2.5) is evaluated and performed in practice by expanding (2.5) around the minimizing field $\boldsymbol{Q}^{\mathcal{G}}(\boldsymbol{r})$. The leading zeroth-order term of this expansion is referred to as the mean-field approximation (MFA). The next-to-leading terms of the expansion are called one-loop, two-loop, etc. approximations. The $\boldsymbol{Q}^{\mathcal{G}}(\boldsymbol{r})$ configuration is also known as a "saddle point" of the Feynman integral (2.1). It is found in practice by minimizing the functional (2.5) over all trial periodic and quasiperiodic fields $\boldsymbol{Q}(\boldsymbol{r})$. The corresponding mean-field expression for the free energy (2.1) is obtained by the substitution $\boldsymbol{Q}(\boldsymbol{r}) = \boldsymbol{Q}^{\mathcal{G}}(\boldsymbol{r})$ into Eq. (2.5).

Having determined an approximate form for the saddle

point configuration and for the mean-field free energy of the system one can proceed with calculations of the phase diagrams and of the phase biaxiality. The latter is reduced to a simpler expression, namely,

$$B = \frac{\int d^3\boldsymbol{x}\,(\{\mathrm{tr}[(\boldsymbol{Q}^{\mathcal{G}})^2]\}^3 - 6\,\{\mathrm{tr}[(\boldsymbol{Q}^{\mathcal{G}})^3]\}^2)}{\int \mathrm{d}^3\boldsymbol{x}\,\{\mathrm{tr}[(\boldsymbol{Q}^{\mathcal{G}})^2]\}^3}. \tag{2.6}$$

Interestingly, for chiral liquid crystals, where $\kappa \neq 0$, even for $\varepsilon' \geq 0$ the phase biaxiality usually is greater than zero, because it is induced by spatial inhomogeneities of equilibrium structures, which may remove the degeneracy of the eigenvalues of $\boldsymbol{Q}(\boldsymbol{r})$. At first sight it may seem difficult to obtain large biaxialities as result of such deformations. Indeed, for small κ and for the model (2.4), the inhomogeneity of, for example, the cholesteric phase induces only a slight and generally unimportant degree of biaxiality. But this is not always the case. As we shall demonstrate in Sec. IV, a large biaxiality may result from the presence of competing bulk terms in the expansion (2.5).

To understand how biaxiality arises for cubic and icosahedral structures note that due to symmetry-imposed restrictions on $\boldsymbol{Q}$ such states are, in general, characterized by a nonzero density of uniaxial prolate and oblate lines and by $\mathrm{tr}\boldsymbol{Q}(\boldsymbol{r}) \neq 0$ (except maybe of an isolated set of points). Consequently these structures may acquire a large degree of biaxiality due to the presence of lines of maximal biaxiality, which are located between the uniaxial prolate and the uniaxial oblate lines [14].

III. MEAN-FIELD FREE-ENERGY CALCULATIONS

Our objective now is to explicitly write down the mean-field free energy (2.1) with $\mathcal{F}$ given by $\mathcal{F}_{\mathrm{EdeGL}}$, Eq. (2.5). In practice the problem reduces to finding a functional minimum of $\mathcal{F}_{\mathrm{EdeGL}}$ for arbitrary κ and T and for fixed values of the material parameters. As already mentioned before, the global minimization in the presence of the chiral term ($\kappa \neq 0$) is practically impossible. Thus the standard procedure is to assume that $\boldsymbol{Q}(\boldsymbol{r})$ is invariant under the action of symmetry operators of a space group $\mathcal{G}$. This yields trial periodic and quasiperiodic states for the equilibrium structures. Clearly, the best approximation $\boldsymbol{Q}^{\mathcal{G}}(\boldsymbol{r})$ to the equilibrium structure is the one with the lowest free energy (2.5)

$$F([\boldsymbol{Q}]) \underset{\mathrm{MFA}}{=} \underset{\{\mathcal{G}\}}{\mathrm{Min}}\ \mathcal{F}_{\mathrm{EdeGL}}\{[\boldsymbol{Q}^{\mathcal{G}}(\boldsymbol{r})]\}. \tag{3.1}$$

The above program is realized in practice by expanding $\boldsymbol{Q}^{\mathcal{G}}(\boldsymbol{r})$ into plane waves of definite helicity

$$\boldsymbol{Q}^{\mathcal{G}}(\boldsymbol{r}) = \sum_{{}^*\boldsymbol{k}} \frac{1}{\sqrt{N_{{}^*\boldsymbol{k}}}} \left[\sum_{\boldsymbol{k}\in{}^*\boldsymbol{k}} \sum_{m=-2}^{2} Q_m(|{}^*\boldsymbol{k}|)\exp(\mathrm{i}\,\boldsymbol{k}\cdot\boldsymbol{r} - \mathrm{i}\,\psi_{\mathrm{m},\hat{\boldsymbol{k}}})\,\boldsymbol{e}^{[2]}_{\mathrm{m},\hat{\boldsymbol{k}}} \right]. \tag{3.2}$$

Here $\boldsymbol{k}$ is taken out of a reciprocal lattice of a space group $\mathcal{G}$, where ${}^*\boldsymbol{k} = \{\boldsymbol{k}' : \boldsymbol{k}' = S\boldsymbol{k}, \{S|\boldsymbol{t}\} \in \mathcal{G}\}$ is the star of $\boldsymbol{k}$, $N_{{}^*\boldsymbol{k}}$ is the number of prongs of the star ${}^*\boldsymbol{k}$, $Q_m(|\boldsymbol{k}|)$ are the variational parameters in the expansion, and finally

$$\begin{aligned}
\boldsymbol{e}^{[2]}_{0,\hat{\boldsymbol{k}}} &= \frac{1}{\sqrt{6}}\left\{3\hat{\boldsymbol{k}}\otimes\hat{\boldsymbol{k}} - \mathbf{1}\right\},\\
\boldsymbol{e}^{[2]}_{\pm1,\hat{\boldsymbol{k}}} &= \pm\frac{1}{2}\left\{(\hat{\boldsymbol{v}} \pm \mathrm{i}\hat{\boldsymbol{w}})\otimes\hat{\boldsymbol{k}} + \hat{\boldsymbol{k}}\otimes(\hat{\boldsymbol{v}} \pm \mathrm{i}\hat{\boldsymbol{w}})\right\},\\
\boldsymbol{e}^{[2]}_{\pm2,\hat{\boldsymbol{k}}} &= \frac{1}{2}\left\{(\hat{\boldsymbol{v}} \pm \mathrm{i}\hat{\boldsymbol{w}})\otimes(\hat{\boldsymbol{v}} \pm \mathrm{i}\hat{\boldsymbol{w}})\right\}
\end{aligned} \tag{3.3}$$

are the spin $L = 2$ tensors represented in an orthogonal, right-handed local coordinate system $\left\{\hat{\boldsymbol{v}}, \hat{\boldsymbol{w}}, \hat{\boldsymbol{k}}\right\}$ with $\hat{\boldsymbol{k}}$ as quantization axis. The reality condition $\boldsymbol{Q}(\boldsymbol{r}) = [\boldsymbol{Q}(\boldsymbol{r})]^*$ additionally implies that

$$\boldsymbol{e}^{[2]}_{m,-\hat{\boldsymbol{k}}} = (-1)^m \left(\boldsymbol{e}^{[2]}_{m,\hat{\boldsymbol{k}}}\right)^* \tag{3.4}$$

and

$$\psi_{m,\hat{\boldsymbol{k}}} + \psi_{m,-\hat{\boldsymbol{k}}} = \pm m\pi. \tag{3.5}$$

The selection of the wave vectors $\boldsymbol{k}$, the phases $\psi_{m,\hat{\boldsymbol{k}}}$, and m is fixed by the symmetry $\mathcal{G}$ of the structure.

Using the parametrization (3.2) the various terms entering the free energy (3.1) can now be written as

$$\begin{aligned}
\frac{1}{4v}\int d^3\boldsymbol{x}\,[T\,\mathrm{tr}(\boldsymbol{Q}^2) - 2\kappa\,\varepsilon_{ijk}\,Q_{in}\,Q_{jn,k} + (Q_{ij,l})^2 + \rho\,Q^2_{ij,j}] = \frac{1}{4}\sum_{{}^*\boldsymbol{k},m}\Bigg\{T - \kappa\,m\,|{}^*\boldsymbol{k}|\\
+\left[1 + \frac{1}{6}\rho\,(4 - m^2)\right]|{}^*\boldsymbol{k}|^2\Bigg\}Q^2_m(|{}^*\boldsymbol{k}|)
\end{aligned} \tag{3.6}$$

and

$$v^{-1}\int d^3\boldsymbol{x}\,[\mathrm{tr}(\boldsymbol{Q}^2)]^p\,[\mathrm{tr}(\boldsymbol{Q}^3)]^q = \sum_{m_1,{}^*k_1}\cdots\sum_{m_{2p+3q},{}^*k_{2p+3q}} \Phi_{\mathcal{G}}({}^*k_1\cdots{}^*k_{2p+3q}; m_1\cdots m_{2p+3q})\left(\prod_{j=1}^{2p+3q} Q_{m_j}(|{}^*\boldsymbol{k}_j|)\right), \tag{3.7}$$

where the space group dependent numerical coefficients $\Phi_{\mathcal{G}}$ are given by

$$\Phi_{\mathcal{G}}({}^*\boldsymbol{k}_1 \cdots {}^*\boldsymbol{k}_{2p+3q}; m_1 \cdots m_{2p+3q}) = \left(\prod_{i=1}^{2p+3q} \frac{1}{\sqrt{N_{{}^*\boldsymbol{k}_i}}}\right) \sum_{\boldsymbol{k}_1 \in {}^*\boldsymbol{k}_1} \cdots \sum_{\boldsymbol{k}_{2p+3q} \in {}^*\boldsymbol{k}_{2p+3q}} \delta\left(\sum_{j=1}^{2p+3q} \boldsymbol{k}_j\right) \exp\left(-i \sum_{l=1}^{2p+3q} \psi_{m_l,\hat{\boldsymbol{k}}_l}\right)$$
$$\times \left[\prod_{i=1}^{n_1} \mathrm{tr}\left(\boldsymbol{e}^{[2]}_{m_{2i-1},\hat{\boldsymbol{k}}_{2i-1}} \boldsymbol{e}^{[2]}_{m_{2i},\hat{\boldsymbol{k}}_{2i}}\right)\right] \left[\prod_{j=n_1+1}^{n_1+n_2} \mathrm{tr}\left(\boldsymbol{e}^{[2]}_{m_{3j-2},\hat{\boldsymbol{k}}_{3j-2}} \boldsymbol{e}^{[2]}_{m_{3j-1},\hat{\boldsymbol{k}}_{3j-1}} \boldsymbol{e}^{[2]}_{m_{3j},\hat{\boldsymbol{k}}_{3j}}\right)\right]. \tag{3.8}$$

The minimization over fields $\boldsymbol{Q}(\boldsymbol{r})$ is thus reduced to a minimization over the real amplitudes $Q_m(|\boldsymbol{k}|)$. The most difficult part of the calculations is finding the $\Phi_{\mathcal{G}}$ coefficients, Eq. (3.8), of the polynomial (3.7), especially for the fifth- and the sixth-order terms of the expansion (2.5). Due to these limitations we restrict the expansion (3.2) to two leading stars $({}^*\boldsymbol{k}_1, {}^*\boldsymbol{k}_2)$ of the $\boldsymbol{k}$ vectors. For each ${}^*\boldsymbol{k}$ we select $m = 2$ modes, corresponding to the low-lying branch of the excitation spectrum of the quadratic part of the free energy (3.6). The last approximation makes $Q_{ij,i}$ vanish and, consequently, the parameter ρ, weighting $(Q_{ij,i})^2$, is redundant.

With these simplifications the two-star mean-field free energy (3.1) of chiral liquid crystals reads

$$\mathcal{F}_{G\mathrm{deGL}}\{[\boldsymbol{Q}(\boldsymbol{r})]\} = \frac{1}{4} \sum_{{}^*\boldsymbol{k},m} \left\{T - \kappa m|{}^*\boldsymbol{k}| + \left[1 + \frac{1}{6}\rho(4 - m^2)\right] |{}^*\boldsymbol{k}|^2\right\} [Q_m(|{}^*\boldsymbol{k}|)]^2 + \beta \sum_{\substack{i,j=0 \\ i+j=3}}^{3} C^3_{ij}\, Q^i_1\, Q^j_2$$
$$+\gamma \sum_{\substack{i,j=0 \\ i+j=4}}^{4} C^4_{ij}\, Q^i_1\, Q^j_2 + \phi \sum_{\substack{i,j=0 \\ i+j=5}}^{5} C^5_{ij}\, Q^i_1\, Q^j_2 + \varepsilon \sum_{\substack{i,j=0 \\ i+j=6}}^{6} C^6_{ij}\, Q^i_1\, Q^j_2 + \varepsilon' \sum_{\substack{i,j=0 \\ i+j=6}}^{6} C^{6'}_{ij}\, Q^i_1\, Q^j_2, \tag{3.9}$$

TABLE I. Two-star bulk contributions to the free energy Eq. (3.9) for various symmetry allowed structures. The contribution proportional to ε is equal to B. The symbols used for the cubic space groups are consistent with the Schönflies notation while the icosahedral space group notation agrees with that introduced by Rokhsar *et al.* [17]. Note that out of 15 possible icosahedral space groups P532, F532, I532, P5$_n$32, F5$_n$32, and I5$_n$32, where n=1,2,3,4, only six icosahedral structures give distinct free energies.

					Structure					
(i,j)	C	O^8	O^2	O^5	F532	F5$_1$32	F5$_2$32	F5$_3$32	F5$_4$32	P5$_2$32
					Third-order coefficients C^3_{ij}					
(3,0)	1.0000	-0.6250	-1.0165	-1.0165	-0.4375	-0.0075	0.4496	-0.7200	0.7154	0.4496
(2,1)		2.1857			-1.5654	-1.5654	-1.5654	-1.5654	-1.5654	
(1,2)	-3.0000		3.0910		1.1161	-0.8898	0.3237	0.3661	-0.9160	-2.8249
					Fourth-order coefficients C^4_{ij}					
(4,0)	1.0000	1.1693	1.2995	1.2995	1.2000	1.1504	1.3536	1.5288	1.4339	1.3536
(3,1)		-1.0009			0.4648	-0.1702	-0.1893	0.4766	-0.5818	
(2,2)	2.0000	3.4994	2.5423		3.1656	3.3911	3.9979	3.0339	3.0072	3.9728
(1,3)					-0.0457	0.8136	0.0399	-0.8865	0.0788	
(0,4)	1.0000	1.0833	1.0833		1.3240	1.4607	1.2740	1.4573	1.3173	1.2333
					Fifth-order coefficients C^5_{ij}					
(5,0)	0.1667	-0.1536	-0.2449	-0.2449	-0.1154	0.0096	0.1118	-0.2736	0.2141	0.1119
(4,1)		0.6243			-0.4676	-0.3790	-0.5772	-0.5652	-0.5740	
(3,2)	-0.3333	-0.4852	0.4961		-0.0191	-0.2847	0.2982	-0.0733	0.1561	-1.0323
(2,3)		0.6236			-0.5099	-0.7216	-0.7214	-0.6094	-0.5187	
(1,4)	-0.5000		0.6158		0.3710	-0.4344	0.0981	0.2349	-0.2919	-0.8002
(0,5)					0.0073	-0.0223	-0.0040	-0.0152	0.0044	
					Sixth-order coefficients C^6_{ij}					
(6,0)	0.1667	0.2548	0.3150	0.3150	0.2712	0.2434	0.3558	0.5310	0.4228	0.3559
(5,1)		-0.5402			0.2964	-0.1130	-0.0870	0.5428	-0.4622	
(4,2)	0.5000	1.4837	0.8757		1.3483	1.3791	2.2092	1.5777	1.5056	2.0790
(3,3)		-0.7069			0.3874	0.4957	-0.0937	-0.3816	-0.4736	
(2,4)	0.5000	1.3573	0.7973		1.4306	1.8906	2.0640	1.5172	1.3435	1.9682
(1,5)					-0.0287	0.6843	0.0425	-0.6918	0.0495	
(0,6)	0.1667	0.2037	0.2037		0.3486	0.4681	0.3165	0.4673	0.3510	0.2885
					Sixth-order coefficients $C^{6'}_{ij}$					
(6,0)		0.0925	0.0214	0.0214	0.1305	0.1251	0.1991	0.1181	0.1664	0.1991
(5,1)		0.2582			-0.2003	0.1153	0.3863	-0.3271	0.4302	
(4,2)	1.5000	-0.1292	2.2936		0.4470	0.2945	0.6611	0.4751	0.2514	1.8192
(3,3)		-0.2285			1.0651	-0.9172	0.3521	0.0363	-1.1126	
(2,4)	-1.0000	1.0292	-1.2560		0.8034	0.8545	1.2182	0.6799	0.9720	-0.8406
(1,5)					-0.0187	0.4291	0.1515	-0.4286	0.0650	
(0,6)	0.1667	0.1829	0.1829		0.1859	0.2999	0.2179	0.3385	0.2305	0.1985

where $Q_1 = Q_2(|{}^*\boldsymbol{k}_1|)$ and $Q_2 = Q_2(|{}^*\boldsymbol{k}_2|)$. With (3.9) the free energies have been calculated explicitly for cholesteric liquid crystals BPI and BPII and for all icosahedral space groups. In the latter case the reciprocal wave vectors were constructed as linear combinations of six integrally independent vertex vectors. The following rules were additionally taken into account: for a primitive reciprocal lattice all integral coordinates were allowed while for a face-centered reciprocal lattice the sum of the coordinates of a vector was taken even. For a body-centered reciprocal lattice all coordinates were assumed to be of the same parity.

A key criterion in selecting the supplementary star of the $\boldsymbol{k}_2$ vectors was to require a maximal number of triangles with the leading star and to keep the ratio $|{}^*\boldsymbol{k}_2|/|{}^*\boldsymbol{k}_1|$ small. Observing correctly the selection rules we arrived at six different icosahedral structures compatible with the (532) point symmetry. Five of these structures are associated with the face-centered space group symmetries F(B)5_n32 ($n = 0, ..., 4$) of ratio $|{}^*\boldsymbol{k}_2|/|{}^*\boldsymbol{k}_1| \approx 1.17$. The last one corresponds to a primitive P5_232 symmetry with $|{}^*\boldsymbol{k}_2|/|{}^*\boldsymbol{k}_1| \approx 1.06$. More specifically, for the P5_232 symmetry ${}^*\boldsymbol{k}_1$ are the vertex vectors and ${}^*\boldsymbol{k}_2$ are the edge vectors of an icosahedron. For the F5_n32 symmetry the representative of the ${}^*\boldsymbol{k}_1$ vectors has coordinates $(2,0,0,-1,0,-1)$ and that of the ${}^*\boldsymbol{k}_2$ vectors corresponds to the $(0,0,1,0,0,1)$ vector of the reciprocal lattice. The notation for icosahedral space groups used above is consistent with that of Rokshar *et al.* [17]. More details are given in the Appendix.

For all space groups involved the numerical coefficients C^l_{ij}, Eq. (3.9), were found by combining group theoretical methods, computer algebra, and numerical techniques. All the nonzero coefficients are listed in Table I.

IV. RESULTS

The minimization of $\mathcal{F}_{\text{EdeGL}}$, Eq. (3.9), was carried out numerically for each trial structure separately at fixed values of chirality and temperature and of the remaining model parameters by using a combination of simplex- and gradient search methods. To ensure that the global minimum was found the procedures were initialized at different points of the $\{Q_1, Q_2\}$ space. The equilibrium free energy and consequently the equilibrium structure was next identified by comparing the free energies of the trial structures at the same values of the thermodynamic and material parameters.

To start the analysis we discuss a simpler case of $\phi = \varepsilon = \varepsilon' = 0$, which corresponds to the original de Gennes–Ginzburg–Landau theory. In this case the (κ, T) plane phase diagram is universal as the term proportional to ρ vanishes for tensor fields composed exclusively of $m = 2$ Fourier components. As shown in Fig. 1, the structures that minimize the free energy (2.4) are predominantly the cholesteric, the O^2 and the O^5 phase, in agreement with a similar analysis carried out before by Grebel *et al.* [12]. Additionally, in a very limited range of the (κ, t) parameters, the O^8 structure is found to be absolutely stable. However, no stable icosahedral structure exists,

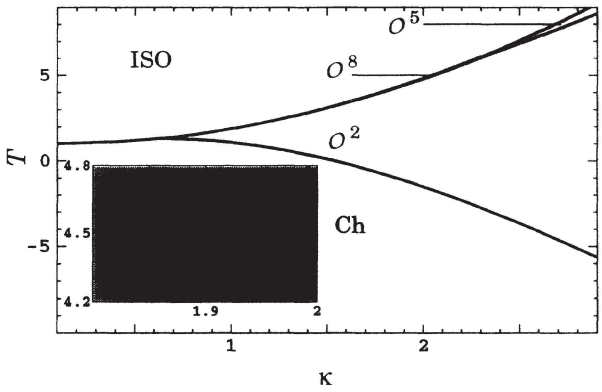

FIG. 1. Phase diagram (chirality, temperature) [$\equiv (\kappa,T)$] calculated for $\beta = \gamma = 1$ and $\phi = \varepsilon = \varepsilon' = 0$. Symbols used for the cubic space groups are consistent with the Schönflies notation. Additionally, ISO denotes the isotropic phase and Ch denotes the cholesteric phase.

although they all could be made more stable than the isotropic liquid. This is again in agreement with earlier, less general, calculations [6,7].

These results can be correlated with the phase biaxialities of the structures; see Figs. 2–5. The plots refer to that part of the (κ, T) plane where a given phase appears more stable than the isotropic liquid. As the biaxiality of the O^5 structure is model independent and equals 0.068, the corresponding diagram is omitted. In the case of icosahedral structures only the biaxiality of the most stable structure is shown. This is the reason for discontinuities in Fig. 5, which indicate that different icosahedral structures become relevant in the admitted

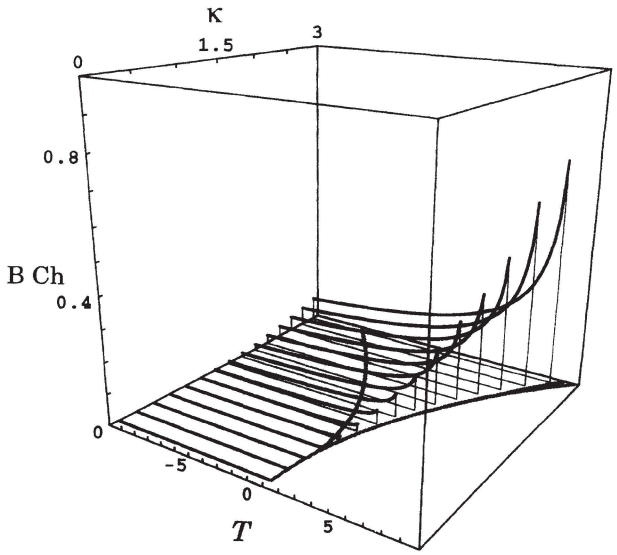

FIG. 2. Chirality and temperature variation of the phase biaxiality $B \equiv B$ Ch, [Eq. (2.3)] for the cholesteric phase. The set of parameters used is the same as in Fig. 1. To visualize a connection between the phase diagram and the phase biaxiality the former has additionally been inserted into the (κ, T) plane.

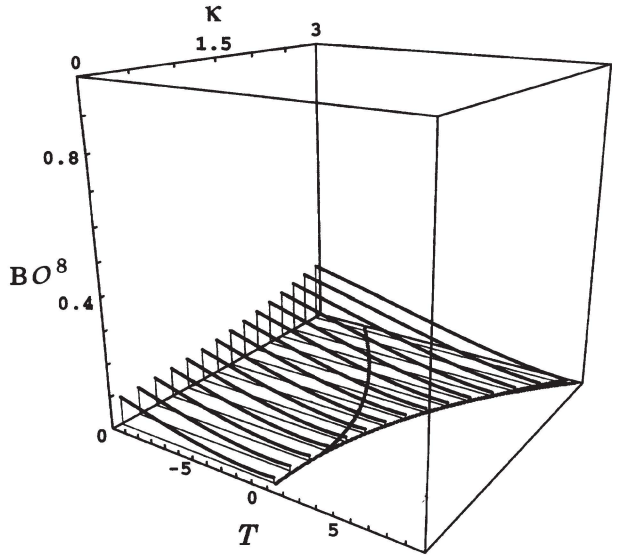

FIG. 3. Chirality and temperature variation of the phase biaxiality $B \equiv BO^8$ [Eq. (2.3)] for the BPI structure modeled by the cubic space group O^8. The set of parameters used is the same as in Fig. 1. To visualize a connection between the phase diagram and the phase biaxiality the former has additionally been inserted into the (κ, T) plane.

range of the thermodynamic parameters. Additionally the phase diagram has been inserted in the (κ, T) plane of Figs. 2–5.

By inspecting Figs. 2–5 one finds that apart from the $F5_332$ structure, all other icosahedral structures are strongly biaxial. The least biaxial are the O^5 and the O^2 structure. These results, when compared with the location of the stable phase on the phase diagram, clearly support the empirical rule that phases of lower biaxiality generally become more stable.

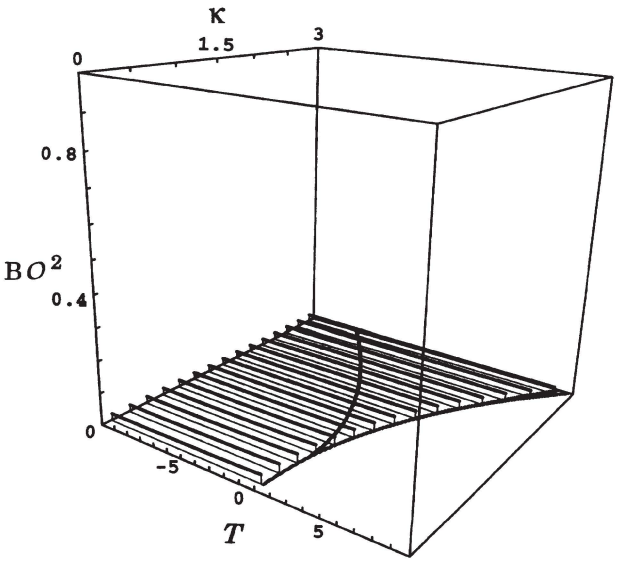

FIG. 4. Chirality and temperature variation of the phase biaxiality $B \equiv BO^2$ [Eq. (2.3)] for the BPII structure modelled by the cubic space group O^2. The set of parameters used is the same as in Fig. 1. To visualize a connection between the phase diagram and the phase biaxiality the former has additionally been inserted into the (κ, T) plane.

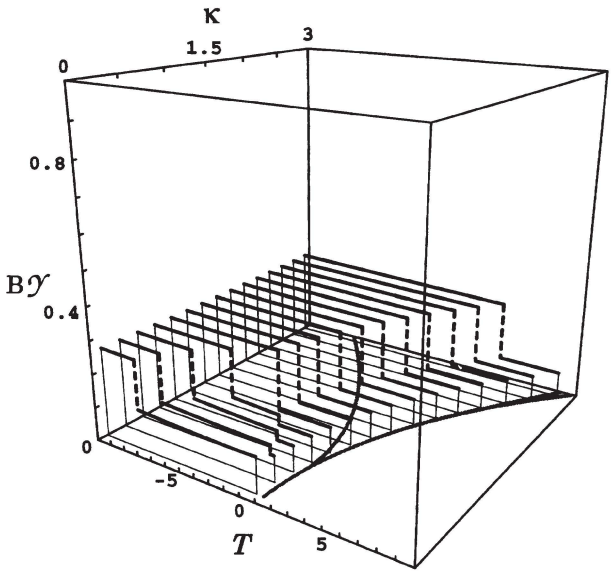

FIG. 5. Chirality and temperature variation of the phase biaxiality $B \equiv BY$ [Eq. (2.3)] for icosahedral structures. The set of parameters used is the same as in Fig. 1. For given (κ, T) only the phase biaxiality of the most stable icosahedral structure (i.e., having the smallest free energy) is shown. Discontinuities (broken lines) of the BY surface separate the most stable, different icosahedral phases. These are, in order of decreasing BY, F532, $P5_232$, and $F5_332$. To visualize a connection between the phase diagram and the phase biaxiality the former has additionally been inserted into the (κ, T) plane.

A similar rule holds approximately for the $\mathcal{F}_{\text{EdeGL}}$ model provided that all material parameters are greater than zero. In this sector of the parameters the phase diagrams are characterized by a high degree of universality. Most of them are similar to the one shown in Fig. 1, although cases without the O^5 or the O^8 structure also have been found.

The third and the fifth degree invariants of the $\mathcal{F}_{\text{EdeGL}}$ are related to the average molecular shape [8]. The corresponding parameters β and ϕ are thus expected to have the same sign in the majority of single-component liquid crystalline materials and the opposite signs in mixtures composed of oblate and prolate molecules. From a theoretical point of view the latter case is quite interesting as it introduces a competition between the oblate and the prolate symmetries. The effect of this competition should lead to a peak (or discontinuity) in the temperature variation of the biaxiality parameter. Indeed, explicit calculations involving many cases with positive β and negative ϕ fully support these expectations. Furthermore, another phenomenon, related to this competition, is found. It involves reentrant phase transitions between the cholesteric phase and the cubic blue phases [see Figs. 6–12] and phase transitions between phases of the same symmetry. The biaxiality parameter serves here as

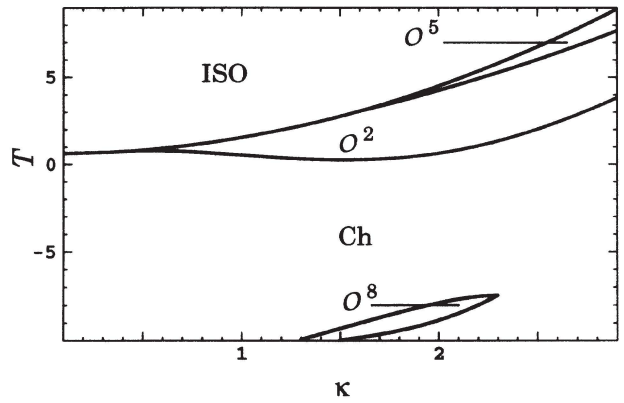

FIG. 6. Phase diagram (chirality, temperature) [$\equiv (\kappa, T)$] calculated for $\beta = \gamma = 1$, $\phi = -10$, $\varepsilon = 10$, and $\varepsilon' = 0$. For definitions of the symbols used see the caption to Fig. 1.

an extra order parameter and allows one to detect first-order phase transitions between structures of the same symmetry. They are seen as discontinuities of B.

The phase transitions between phases of the same symmetry are easily realized in practice. Take, for example, a set of the material parameters which, for $\kappa = 0$, give a first-order phase transition between the uniaxial and the biaxial nematic phases. For small nonzero values of κ, the nematic phases are replaced by the cholesteric ones, both of the same symmetry but of different biaxialities, with a first-order phase transition separating them. With increasing chirality a critical point is eventually approached and the whole (B, κ, T) diagram resembles that of a conventional gas-liquid transition. In this case a typical behavior of B follows the one shown in Fig. 9.

The appearance of the reentrant phase transitions is less obvious. They are found when both the competition between the β and the ϕ terms are present and the already discussed "rule of smaller biaxiality" is approximately fulfilled. Then at low temperatures, when the order parameters are large, the stable (quasi-)periodic structure is likely to be that which minimizes the fifth-order term. However, the situation is reversed at higher

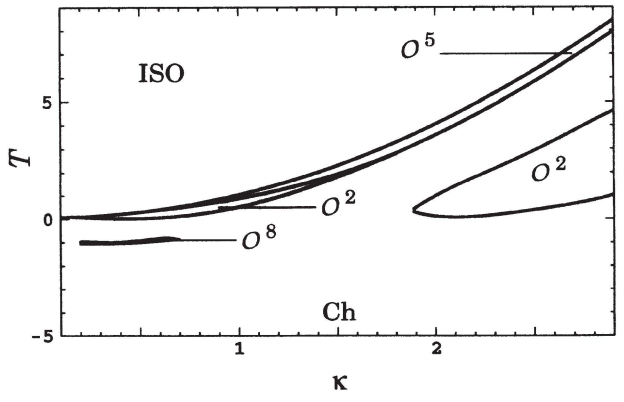

FIG. 7. Phase diagram (chirality, temperature) [$\equiv (\kappa, T)$] calculated for $\beta = \gamma = 0.1$, $\phi = -1$, $\varepsilon = 1$, and $\varepsilon' = 0$. For definitions of the symbols used see the caption to Fig. 1.

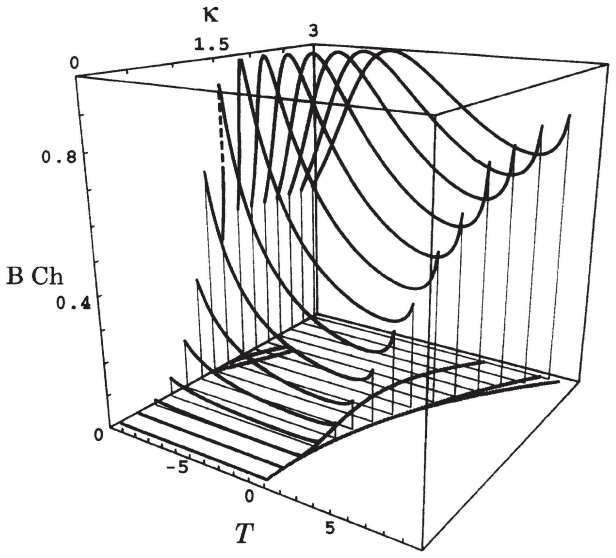

FIG. 8. Chirality and temperature variation of the phase biaxiality $B \equiv B$ Ch [Eq. (2.3)] for the cholesteric phase. The set of parameters used is the same as in Fig. 6. Phase biaxialities for the case shown in Fig. 7 are similar. To visualize a connection between the phase diagram and the phase biaxiality the former Fig. (6) has additionally been inserted into the (κ, T) plane.

temperatures, especially in the vicinity of the isotropic phase, where the cubic term is the one that should be minimized. If the low and the high temperature phases are of the same symmetry, then, because of these competing tendencies of the fifth-order and the cubic terms, there is an intermediate temperature where the phase bi-

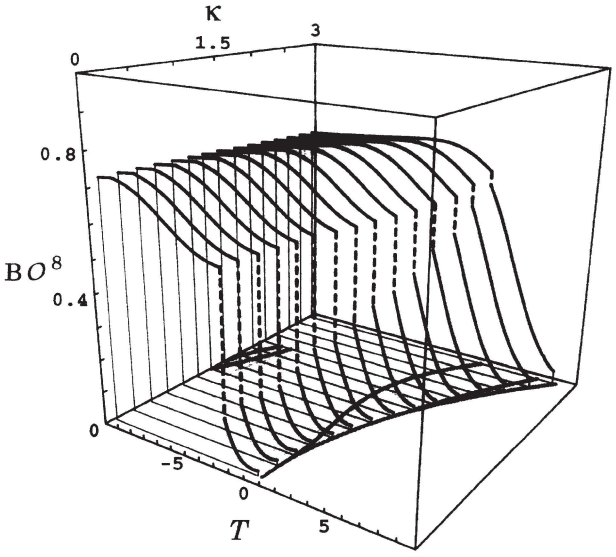

FIG. 9. Chirality and temperature variation of the phase biaxiality $B \equiv B\,O^8$ [Eq. (2.3)] for the BPI structure modeled by the cubic space group O^8. The set of the parameters used is the same as in Fig. 6. Phase biaxialities for the case shown in Fig. 7 are similar. To visualize a connection between the phase diagram and the phase biaxiality the former (Fig. 6) has additionally been inserted into the (κ, T) plane.

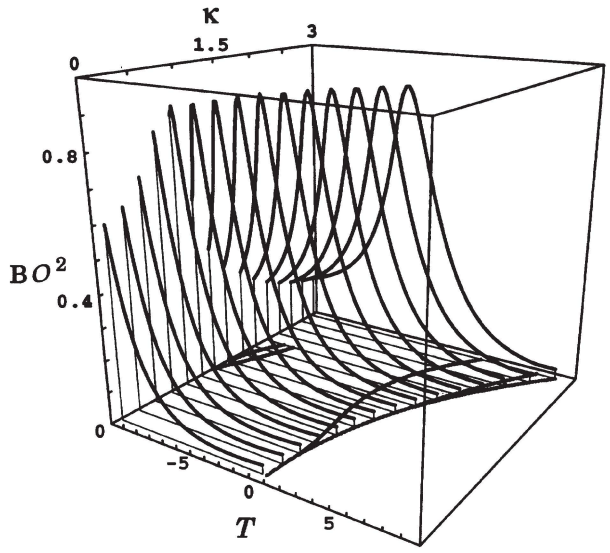

FIG. 10. Chirality and temperature variation of the phase biaxiality $B \equiv BO^2$ [Eq. (2.3)] for the BPII structure modeled by the cubic space group O^2. The set of parameters used is the same as in Fig. 6. Phase biaxialities for the case shown in Fig. 7 are similar. To visualize a connection between the phase diagram and the phase biaxiality the former (Fig. 6) has additionally been inserted into the (κ,T) plane.

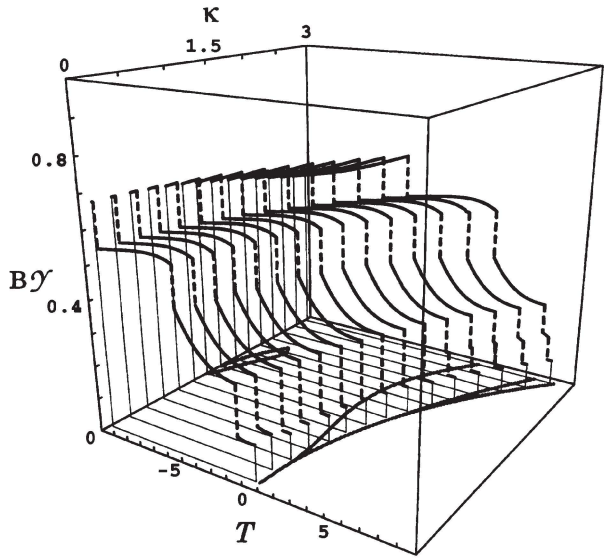

FIG. 11. Chirality and temperature variation of the phase biaxiality $B \equiv BY$ [Eq. (2.3)] for icosahedral structures. The set of parameters used is the same as in Fig. 6. Phase biaxialities for the case shown in Fig. 7 are similar. Again only the phase biaxiality (BY) of the most stable icosahedral structure is shown. As in Fig. 5, discontinuities of BY indicate that different icosahedral phases take over. These are, in order of decreasing BY, F532, F5$_1$32, F532, F5$_4$32, P5$_2$32, and F5$_3$32. Again, for definitions of the symbols used see the caption to Fig. 1. To visualize a connection between the phase diagram and the phase biaxiality the former (Fig. 6) has additionally been inserted into the (κ,T) plane.

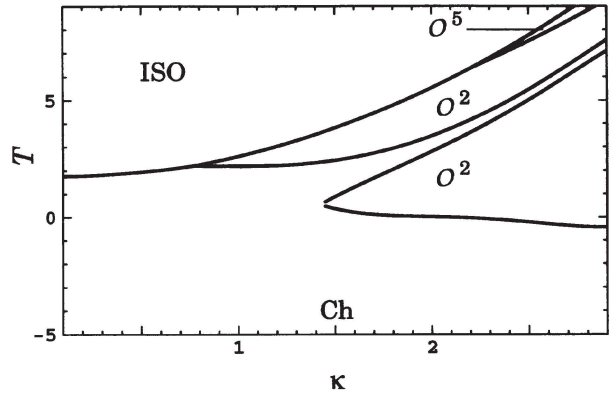

FIG. 12. Phase diagram for $\beta = 1$, $\gamma = -1$, $\phi = -10$, $\epsilon = 10$, and $\epsilon' = 0$. For definitions of the symbols used see the caption to Fig. 1.

axiality is maximal. In these cases, as shown in Figs. 8 and 10, the phase biaxiality may even approach its maximal value equal 1, also in effectively uniaxial liquid crystalline systems. This in turn may stabilize a new, less biaxial phase around the maximal value of B. At higher temperatures (chiralities), where B of the "old" phase is again small, the "old" phase may reenter. This is illustrated in Figs. 6, 8, and 12. Be aware, however, of the fact that the rule of smaller biaxiality is only fulfilled approximately. For example, it does not hold for most of the systems characterized by $\epsilon' < 0$.

The reentrant phenomenon was detected in a wide range of parameters around those of Figs. 6, 7, and 12 indicating a possibility of finding similar behavior in real liquid crystalline systems. For $\epsilon' < 0$ the reentrant behavior was usually eliminated.

Finally, we turn to the problem of stability of an icosahedral structure. The detailed mean-field analysis shows that icosahedral phases may become more stable than some of the cubic structures or the cholesteric phase, but they are never absolutely stable in the admitted (κ, T) range. The results are consistent with those reported earlier [7], which were restricted to an immediate neighborhood of the isotropic phase.

V. SUMMARY AND FINAL DISCUSSION

We have studied the extended de Gennes–Ginzburg–Landau model to answer some of the basic questions concerning chiral liquid crystals. Our intentions were (a) to study the influence of higher-order terms in de Gennes–Ginzburg–Landau theory on stability of chiral phases, (b) to show the importance of the phase biaxiality parameter in the description of equilibrium properties of chiral phases, (c) to identify possible classes of the phase diagrams in the extended de Gennes–Ginzburg–Landau theory, and (d) to analyze in detail the stability of icosahedral structures.

The first question that arises, however, is whether one really should take time and analyze the extended model by including fifth- and sixth-order terms in the order pa-

rameter. After all there exist a few other possible directions in which the standard model [1] could be generalized.

Certainly one reason for studying this extension is to verify whether the standard fourth-order termination is correct. The second reason seems less trivial and it comes, as argued in Ref. [7(b)] [see also Ref. [8(a)]], from the analysis of uniaxial nematics in the vicinity of the nematic-isotropic (NI) phase transition. Namely, it has been demonstrated that the experimental data for nematic liquid crystals fit very well to the model with a sixth-order term being dominant. As the presence of chirality should not change the phenomenological parameters significantly, one may expect for chiral systems the existence of a new physically relevant sector in the extended parameter space, which is not accessible within the standard model. Also biaxial fluctuations are important close to the NI transition, as follows from the statistical field theory for $\kappa = 0$ [8], Eqs. (2.1) and (2.4).

Thus the theory as represented by Eqs. (2.1) and (2.4) could be regarded as a fundamental description of chiral liquid crystals, and the analysis of its ground states is a first step towards more advanced studies. Consequently, our attention was focused to the mean-field calculations. We restricted the expansion of the order parameter to two leading stars of the $\boldsymbol{k}$ vectors. But being aware of the two-star limitations, especially for the BPI structure, we have taken the trouble to work out the phase diagrams and the biaxiality parameter in detail, in the whole parameter space. Such analysis, when treated with caution, seems to yield results that may hold true irrespectively of the number of stars taken.

Detailed studies show that, contrary to the previous two-star calculations [1], all the relevant phases, including bcc, could be found on a single diagram. However, the extended model does not improve the agreement with experiments compared to the four-star calculations of the standard model. Again in all cases studied the O^2, the cholesteric, and the O^5 appear to be the most stable structures, with the O^5 found in the part of the diagram where normally BPIII is present. We did not find a parameter window in which the O^8 is favored over the O^2 as seen in experiments. A high stability of the O^2 and of the O^5, which exists for a wide range of chiralities and of the parameters, is suggesting that this situation cannot really be improved even if more stars are present in the expansion of the tensor field.

Thus it seems unlikely that the mean-field analysis could solve the problem of the relative regions of the phase diagram occupied by the simple cubic and bcc phases and consequently produce a generic phase diagram which is consistent with experiment. This, together with the earlier papers on blue phases, clearly shows that the chiral liquids cannot be fully understood without more advanced, statistical field theory calculations, using Eqs. (2.1) and (2.4). A systematic analysis of the effect of fluctuations has already been undertaken [5]. Further results will be presented in a forthcoming publication.

A fluctuation scenario for chiral phases is even more strongly supported by the presented systematic analysis of all possible icosahedral structures, which, besides the O^5, seem to be the *only* mean-field alternatives for the BPIII. First of all we noted that the fifth-order invariant, in addition to the cubic one, strongly favors icosahedral structures (see Table I). Taking into account the fact that all relevant cubic structures are recovered within the two-star analysis, one may expect that an icosahedral structure should also show up somewhere on the phase diagram. Here again the lack of the temperature-chirality window in which the icosahedral structure is more stable than the cholesteric and the cubic structures not only strongly limits the mean field possibilities for the BPIII but also the mean field itself. Perhaps we should add that the complete four-star calculations of icosahedral structures within the frame of the extended model are, practically speaking, impossible. Already two-star analysis appears quite nontrivial.

For completeness, we should also point out that for some limiting values of the parameters, especially when the cubic term plays no role, some other space groups may become relevant. Unfortunately, the global analysis of the mean-field structures for the extended model is again practically impossible. We therefore restricted ourselves to those phases that seem most relevant to our present understanding of chiral liquid crystals.

Interestingly, through a competition between the cubic, the fifth-order, and the sixth-order terms we found a class of phenomena: (a) large biaxialities in potentially uniaxial systems, (b) the reentrant phase transitions, and (c) the phase transitions between phases of the same symmetry but of different biaxialities.

The validity of these results seems to go beyond the two-star limitations. For example, the reentrance feature appears as a result of an anomalous behavior of the biaxiality parameter of the cholesteric phase. More specifically, when the cubic and the fifth-order couplings are of opposite sign one may detect in the chirality-temperature plane an "island" around which the biaxiality of the cholesteric phase has its maximum (see Fig. 8). This effect is quite common for cholesterics and, of course, independent of the number of stars included in the expansion for the cubic structures. For some values of the couplings a dramatic increase of biaxiality to its maximal value equal to 1 strongly reduces the cubic invariant for the cholesteric phase. This in turn gives a chance for a cubic structure to become more stable within the island than the cholesteric phase (compare Figs. 6 and 8). Inclusion of more stars would certainly lower the free energy of this induced cubic structure with respect to the (unchanged) reference cholesteric free energy. In the first place one would then expect that the area of stability of the induced phase is enhanced. As the temperature distance between the O^8 and the O^2 strongly depends on the parameters of the model (compare Figs. 6 and 7), it seems unlikely that this would eliminate reentrant phenomenon in all cases.

The case of phase transitions between phases of the same symmetry is less obvious and might depend upon the number of stars, in analogy to the case of the bcc blue phase when the number of stars considered was raised from two to three. However, we still expect that at least a direct phase transition between the two bi-

axial cholesteric phases should be observed. Indeed if we take the zero chirality limit we can easily induce a uniaxial nematic-biaxial nematic phase transition, where the phase biaxiality is associated here with an intrinsic (molecular) biaxiality. As the corresponding phase transition is of first order, this sequence is replaced for small chiralities by the first-order phase transition between the two cholesteric phases of the same symmetry. Biaxiality of the high temperature cholesteric phase is small and induced by deformations. On the other hand, the low temperature cholesteric phase is induced by the intrinsic biaxiality (due to the sixth-order term). In other words, the effect results from an interplay between the induced and the intrinsic biaxialities.

ACKNOWLEDGMENTS

This research was supported in part by the Heraeus Foundation and by the Polish Commette for Scientific Research (KBN), Grant No. 2.0254.91.01.

APPENDIX: MEAN-FIELD FREE ENERGIES OF ICOSAHEDRAL STRUCTURES

In this appendix we show how to calculate in a systematic way the mean-field free energy (2.5) for an icosahedral liquid crystal. We use a method of the theory of metallic quasicrystals, where the scalar mass density is viewed as an irrational cut through a six-dimensional hypercubic mass density. This six-dimensional hyperspace is a direct sum space of the physical space $\mathbb{E}^{\parallel}$ and of the orthogonal space $\mathbb{E}^{\perp}$ [15,16].

The wave vectors $\boldsymbol{k} = \boldsymbol{k}^{\parallel}$ are lifted through the six-dimensional space

$$\boldsymbol{\kappa} = \boldsymbol{k}^{\parallel} + \boldsymbol{k}^{\perp} \tag{A1}$$

to span a hypercubic reciprocal lattice. Note that the extension of the reciprocal vectors is given by an irrational cut and therefore is unique. Similarly, the position vector $\boldsymbol{r} = \boldsymbol{r}^{\parallel}$ is extended in a natural way to a six-dimensional position vector

$$\boldsymbol{\xi} = \boldsymbol{r}^{\parallel} + \boldsymbol{r}^{\perp} .$$

Using the properties of the six-dimensional hypercubic reciprocal lattice, the Fourier expansion of a real, periodic quadrupole tensor field in six dimensions can now be written down as

$$\boldsymbol{Q}^{(6)}(\boldsymbol{\xi}) = \sum_{\boldsymbol{k}} \frac{1}{\sqrt{N_{*\boldsymbol{k}}}} \sum_{m=-2}^{2} Q_m(\boldsymbol{k})\, \boldsymbol{e}^{[2]}_{m,\hat{\boldsymbol{k}}}\, e^{i\boldsymbol{\kappa}\cdot\boldsymbol{\xi}} . \tag{A2}$$

The physical, quasiperiodic tensor field $\boldsymbol{Q}(\boldsymbol{r})$ can be recovered from the formula (A2) by making an irrational cut through $\boldsymbol{Q}^{(6)}(\boldsymbol{\xi})$

$$\begin{aligned}\boldsymbol{Q}(\boldsymbol{r}) &\equiv \boldsymbol{Q}^{(6)}(\boldsymbol{\xi})|_{\boldsymbol{r}^{\perp}=0} \\ &= \sum_{\boldsymbol{k}} \frac{1}{\sqrt{N_{*\boldsymbol{k}}}} \sum_{m=-2}^{2} Q_m(\boldsymbol{k})\, \boldsymbol{e}^{[2]}_{m,\hat{\boldsymbol{k}}}\, e^{i\boldsymbol{\kappa}\cdot\boldsymbol{r}^{\parallel}} .\end{aligned} \tag{A3}$$

The unknowns in the last formula are the complex amplitudes $Q_m(\boldsymbol{k})$ and the tensors $\boldsymbol{e}^{[2]}_{m,\hat{\boldsymbol{k}}}$ or, equivalently, the orthogonal right-handed local coordinate systems $\left\{\hat{\boldsymbol{v}}_{\hat{\boldsymbol{k}}}, \hat{\boldsymbol{w}}_{\hat{\boldsymbol{k}}}, \hat{\boldsymbol{k}}\right\}$. This freedom is severely reduced by the fact that $\boldsymbol{Q}^{(6)}$ is a real field, invariant under the action of an icosahedral space group. A systematic procedure is outlined below.

First we note that the reality condition for the tensor field (A3) implies, in addition to (3.4), that

$$\begin{gathered}\left\{\hat{\boldsymbol{v}}, \hat{\boldsymbol{w}}, \hat{\boldsymbol{k}}\right\} \underset{\hat{\boldsymbol{k}}\to-\hat{\boldsymbol{k}}}{\longrightarrow} \left\{\hat{\boldsymbol{v}}, -\hat{\boldsymbol{w}}, -\hat{\boldsymbol{k}}\right\}, \\ Q^{*}_{m}(\mathbf{k}) = (-1)^{m} Q_{m}(-\mathbf{k}),\end{gathered} \tag{A4}$$

where, for the icosahedral symmetries, the reciprocal vectors $-\boldsymbol{k}$ and $\boldsymbol{k}$ belong to the same star $^{*}\boldsymbol{k}$. The restrictions due to the symmetry of $\boldsymbol{Q}^{(6)}$ become evident after applying an arbitrary icosahedral space group element $\{g|\boldsymbol{t}_g\}$ to the six-dimensional tensor field

$$[\{g|\boldsymbol{t}_g\}\boldsymbol{Q}^{(6)}](\boldsymbol{\xi}) = g\,\boldsymbol{Q}^{(6)}(\{g|\boldsymbol{t}_g\}^{-1}\,\boldsymbol{\xi})$$

and assuming that the tensor is left unchanged

$$[\{g|\boldsymbol{t}_g\}\boldsymbol{Q}^{(6)}](\boldsymbol{\xi}) \equiv \boldsymbol{Q}^{(6)}(\boldsymbol{\xi}) .$$

This invariance condition generates a relation between $Q_m(\boldsymbol{k})$ and $\boldsymbol{e}^{[2]}_{m,\hat{\boldsymbol{k}}}$

$$Q_m(g\boldsymbol{k})\, \boldsymbol{e}^{[2]}_{m,g\hat{\boldsymbol{k}}} = Q_m(\boldsymbol{k})\, g\boldsymbol{e}^{[2]}_{m,\hat{\boldsymbol{k}}}\, e^{-i\,g\boldsymbol{\kappa}\cdot\boldsymbol{t}_g} , \tag{A5}$$

which implies that for each star $^{*}\boldsymbol{k}$ only a single (in general complex) amplitude is independent, say, $Q_m(\boldsymbol{k})$. It may be chosen by fixing an arbitrary $\boldsymbol{k}$ vector from the star ($\boldsymbol{k} \in {}^{*}\boldsymbol{k}$). Additionally, by incorporating the complex phase factor of $Q_m(\boldsymbol{k})$ in the tensor $\boldsymbol{e}^{[2]}_{m,\hat{\boldsymbol{k}}}$, the amplitude $Q_m(\boldsymbol{k})$ can be taken to be real, which considerably simplifies the numerical analysis.

The last step of the procedure is to determine the phase factors $g\boldsymbol{\kappa}\cdot\boldsymbol{t}_g$ or, equivalently, the nonprimitive translations $\boldsymbol{t}_g$ of the six-dimensional hypercubic lattice. For that we must supplement the twofold (g_2) and the fivefold (g_5) icosahedral point group generators by the corresponding space group translations $\boldsymbol{t}_{g_2}$ and $\boldsymbol{t}_{g_5}$.

The latter can be written as a superposition of the six basis vectors $\boldsymbol{\kappa}_i$ of the hypercubic reciprocal lattice

$$\boldsymbol{t}_{g_5} = \sum_{i=1}^{6} s_i\, \hat{\boldsymbol{\kappa}}_i, \tag{A6}$$

$$\boldsymbol{t}_{g_2} = \sum_{i=1}^{6} r_i\, \hat{\boldsymbol{\kappa}}_i, \tag{A7}$$

where the coordinates s_i and r_i are, in general, rational numbers. The $\boldsymbol{\kappa}_i$ vectors are connected through the condition (A1) with six (out of the twelve) vertex vectors $\boldsymbol{k}^{\parallel}_i$ of an icosahedron.

By applying the icosahedral space group relations between the generators [17]

$$\{g_5|\boldsymbol{t}_{g_5}\}^5 \equiv \{g_2|\boldsymbol{t}_{g_2}\}^2 \equiv \{g_2\, g_5|g_2\, \boldsymbol{t}_{g_5} + \boldsymbol{t}_{g_2}\}^3 \equiv \{e|\mathbf{0}\}$$

to the vectors (A6) we arrive at the set of conditions for the unknown coordinates s_i and r_i. They read

$$\begin{aligned} s_1 = \frac{c}{5}, \frac{c}{5} \pm 1, \frac{c}{5} \pm 2, \cdots \equiv \frac{c}{5} \bmod 1, \\ s_2 = s_3 = s_4 = s_5 = s_6 \equiv 0 \bmod 1 \end{aligned} \tag{A8}$$

$$\begin{aligned} r_3 = -r_6 = r_4 - r_5 \equiv \frac{c}{5} \bmod 1 \\ r_1 = r_2 \equiv 0 \bmod 1, \end{aligned}$$

where $c = 0, 1, \ldots, 4$.

Now the calculations proceed in a straightforward way. As an example consider the $m = 2$ modes, which are relevant to the calculations presented in this paper. In this case the reality condition of $Q_2(\boldsymbol{k})$ implies that

$$Q_2(\boldsymbol{k}) = Q_2^*(\boldsymbol{k}) \equiv Q_2(-\boldsymbol{k}).$$

Thus one must seek for an icosahedral space group element satisfying the relations

$$\begin{aligned} g\boldsymbol{k} &= -\boldsymbol{k}, \\ \boldsymbol{e}^{[2]}_{2,-\hat{\boldsymbol{k}}} &= g\boldsymbol{e}^{[2]}_{2,\hat{\boldsymbol{k}}}\, e^{i\,\boldsymbol{\kappa}_{\boldsymbol{k}}\cdot\boldsymbol{t}_g} \equiv \boldsymbol{e}^{[2]*}_{2,\hat{\boldsymbol{k}}}\,. \end{aligned} \tag{A9}$$

If such a space group element does not exist, the amplitudes associated with the star are not allowed by symmetry and must be set equal to 0 (extinction rules). If, however, the g element is found, one is now able to determine the corresponding orthonormal tripod

$$\{\hat{\boldsymbol{v}}, \hat{\boldsymbol{w}}, \boldsymbol{k} \equiv \boldsymbol{\kappa}\} \tag{A10}$$

and the numbers s_i, r_i satisfying the relations (A5), (A8), and (A9). All the remaining tensors $\boldsymbol{e}^{[2]}_{m,\hat{\boldsymbol{k}}}$ and the phase factors can be found from (A10) and from the group multiplication table.

[1] For recent reviews see, D. C. Wright and N. D. Mermin, Rev. Mod. Phys. **61**, 385 (1989); P. P. Crooker, Liq. Cryst. **5**, 751 (1989); R. M. Hornreich and S. Shtrikman, Mol. Cryst. Liq. Cryst. **165**, 183 (1988); V. A. Belyakov and V. E. Dmitrienko, Usp. Fiz. Nauk **146**, 369 (1985) [Sov. Phys. Usp. **28**, 535 (1985)].

[2] D. K. Yang and P. P. Crooker, Phys. Rev. A **35**, 4419 (1987).

[3] H. Stegemeyer and K. Bergmann, in *Liquid Crystals of One- and Two-Dimensional Order*, edited by W. Helfrich and G. Heppke (Springer, Berlin, 1980), p. 161.

[4] M. Marcus, J. Phys. (Paris) **42**, 61 (1981).

[5] L. Longa and H.-R. Trebin, Phys. Rev. Lett. **71**, 2757 (1993).

[6] R. M. Hornreich and S.Shtrikman, Phys. Rev. Lett. **56**, 1723 (1986); see also H. Kleinert and K. Maki, Fortschr. Phys. **29**, 219 (1981).

[7] (a) R. M. Hornreich, M. Kugler, and S. Shtrikman, Phys. Rev. Lett. **54**, 2099 (1985); (b) L. Longa, W. Fink, and H.-R. Trebin, Phys. Rev. E **48**, 2296 (1993).

[8] (a) See, e.g., F. Gramsbergen, L. Longa, and W. H. de Jeu, Phys. Rep. **135**, 195 (1986), and references therein; (b) L. Longa, Liq. Cryst. **5**, 443 (1989); (c) for a general discussion of higher-order expansions in terms of $Q_{\alpha\beta}(\boldsymbol{r})$ see, e.g., L. Longa and H.-R. Trebin, Phys. Rev. A **39**, 2160 (1989); **42**, 3453 (1990).

[9] D. Shechtman, I. Blech, D. Gratias, and J. W. Cahn, Phys. Rev. Lett. **53**, 1951 (1984).

[10] P. G. de Gennes, *The Physics of Liquid Crystals* (Clarendon, Oxford, 1974).

[11] H. Grebel, R. M. Hornreich, and S. Shtrikman, Phys. Rev. A **28**, 1114 (1983); **30**, 3264 (1984); L. Longa, D. Monselesan, and H.-R. Trebin, Liq. Cryst. **4**, 769 (1989).

[12] The case studied by Grebel *et al.* [11] corresponds to the assignment $\beta = 1, \gamma = 1$, and $\phi = \varepsilon = \varepsilon' = 0$.

[13] Though β and γ are redundant in the present case, we shall keep them explicitly in the expansion (2.4) since they become relevant when higher order terms are included in (2.4).

[14] M. Kiemes, Ph.D. thesis, University of Stuttgart, 1991.

[15] H.-R. Trebin, W. Fink, and H. Stark, J. Phys. I **1**, 1451 (1991).

[16] H.-R. Trebin, W. Fink, and H. Stark, Int. J. Mod. Phys. B **7**, 1475 (1993).

[17] D. S. Rokhsar, D. C. Wright, and N. D. Mermin, Phys. Rev. B **3**, 8145 (1988).

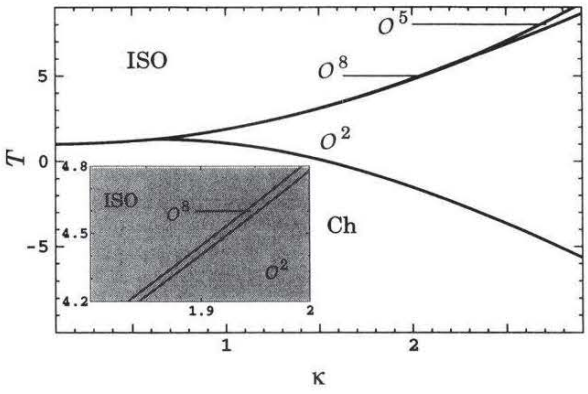

FIG. 1. Phase diagram (chirality, temperature) [$\equiv (\kappa,T)$] calculated for $\beta = \gamma = 1$ and $\phi = \varepsilon = \varepsilon' = 0$. Symbols used for the cubic space groups are consistent with the Schönflies notation. Additionally, ISO denotes the isotropic phase and Ch denotes the cholesteric phase.